An optimal energy management system for islanded Microgrids based on multi-period artificial bee colony combined with Markov Chain

Marzband, Mousa; Azarinejadian, Fatemeh; Savaghebi, Mehdi; Guerrero, Josep M.

Published in:
I E E E Systems Journal

DOI (link to publication from Publisher):
10.1109/JSYST.2015.2422253

Publication date:
2017

Document Version
Early version, also known as pre-print

An optimal energy management system for islanded Microgrids based on multi-period artificial bee colony combined with Markov Chain

Mousa Marzband, Fatemeh Azarinejadian, Mehdi Savaghebi, Member, IEEE, and Josep M. Guerrero, Fellow, IEEE

***Abstract*—Optimal operation programming of electrical systems through minimization of production cost and market clearing price (MCP) as well as better utilization of renewable energy resources has attracted the attention of many researchers. To reach this aim, energy management systems (EMS) has been studied in many research activities. Moreover, demand response (DR) expands customer participation to power systems and results in a paradigm shift from conventional to interactive activities in power systems due to the progress of smart grid technology. Therefore, modelling of consumer characteristic in DR is becoming so important issues in these systems. The customer information as the registration and participation information of DR is used to provide additional indices for evaluating customer response, such as consumer′s information based on the offer priority, DR magnitude, duration, and minimum cost of energy (COE). In this paper, a multi-period artificial bee colony (MABC) optimization algorithm is implemented for economic dispatch considering generation, storage and responsive load offers. The better performance of the proposed algorithm is shown in comparison with the modified conventional energy management system (MCEMS) and its effectiveness is validated experimentally over a Microgrid (MG) Testbed. The obtained results show cost reduction (by around 30%), convergence speed increase as well as remarkable improvement of efficiency and accuracy under uncertain conditions. An artificial neural network (ANN) combined with Markov-chain (MC) (ANN-MC) approach is used to predict non-dispatchable power generation and load demand considering uncertainties. Furthermore, other capabilities such as extendibility, reliability and flexibility are examined about the proposed approach.**

***Index Terms*—artificial bee colony, demand response, microgrid, Optimum energy management, optimum scheduling of DG, responsive load demand, uncertainty.**

This work was supported by the Energy Technology Development and Demonstration Program (EUDP) through the Sino-Danish Project "Microgrid Technology Research and Demonstration" (meter.et.aau.dk).

M. Marzband is (email: mousa.marzband@manchester.ac.uk) with School of Electrical and Electronic Engineering, Faculty of Engineering and Physical Sciences, Electrical Energy and Power Systems Group, The University of Manchester, Ferranti Building, Manchester, M13 9PL, United kingdom.

M. Marzband (email: m.marzband@liau.ac.ir) and F. Azarinejadian (email: niloofar.azari@yahoo.com) are with Department of Electrical Engineering, Lahijan Branch, Islamic Azad University, Lahijan, Guilan, Iran.

M. Savaghebi and J. M. Guerrero are with the Department of Energy Technology, Aalborg University, DK-9220 Aalborg East, Denmark (email: mes@et.aau.dk , joz@et.aau.dk).

NOMENCLATURE

Acronyms

ABC	artificial bee colony
ANN	artificial neural network
DR	demand response
DSM	demand side management
EGP	excess generated power
EMS	energy management system
ES	energy storage
ES+	ES during charging mode
ES-	ES during discharging mode
EWH	electric water heater
MG	microgrid
LEM	local energy market
MABC	multi-period ABC
MCEMS	modified conventional EMS
MC	Markov-chain
MCP	market clearing price
MLP	multi-layer perceptron
MINLP	mixed integer non-linear programming
MPE	maximum prediction error
MT	micro-turbine
NRL	non-responsive load
PSO	particle swarm optimization
PV	photovoltaic
RLD	responsive load demand
SOC	state-of-charge
TPM	transition probability matrix
UP	undelivered power
WT	wind turbine

Variables

π^A	the supply bids by A (€/kWh)
A $\in$ {WT, PV, MT, ES-, ES+, UP, EGP, & EWH}	
λ_t^{MCP}	MCP at each time t in MCEMS (€/kWh)
$\lambda_t'^{MCP}$	MCP at each time t in EMS-MABC (€/kWh)
P_t^A	available power of A in MCEMS (kW)
$P_t'^A$	available power of A in EMS-MABC (kW)
$\tilde{P}_t^A$	real power set-points of A in MCEMS (kW)
$\tilde{P}_t'^A$	real power set-points of A in EMS-MABC (kW)
P_t^A	available power of A (kW)
P_t^n	non-responsive load (NRL) demand (kW)
SOC_t	battery SOC in MCEMS (%)
SOC_t'	battery SOC in EMS-MABC (%)
$\overline{P}$, $\underline{P}$	limit of power (kW)
$\overline{E}$, $\underline{E}$	limit of energy (kWh)

$\overline{SOC}$	maximum SOC (%)
$\underline{SOC}$	minimum SOC (%)
Δt	time step

I. Introduction

FLEXIBILITY requirements in electric power systems and presence of non-dispatchable intermittent generation leads to development of Microgrids (MG)s [1]. An MG can be defined as a small power system consisting of power converter-based generation, energy storage devices, small classic synchronous generation and various types of loads. This configuration with a proper control could provide lots of advantages to consumers such as better power quality, higher reliability, more flexibility, and less operation and generation cost [2]–[5]. Adequate amount of demand side delivery in MGs has significant importance due to limitations of using non-dispatchable resources [6], [7]. The problem of demand-supply mismatch exists in these systems if energy generation resources are not adequate to supply the requested load and no proper EMS is employed. An EMS makes optimal use of available DGs while ensuring the flexibility, reliability and quality of the supply. However, it may also fail to produce the load demand if total demand is more than the total generated power. Under such scenarios, utilizing backup systems such as energy storage (ES), diesel generators or applying demand response (DR) helps to reduce the demand-supply mismatch [8], [9]. At present, ES can be implemented only in small scale and for a short-time supply. Moreover, DR mechanism may leads to reduction of the fluctuations resulting from random and unwanted requests which may help to provide peak shaving [10], [11]. The combined operation of ES and DR with DG technologies provide more reliability for MG operation [8], [9], [12]. Hence, intelligent control systems must be developed to accommodate ES and DR in MGs in order to supply consumers as required [6], [13]. Optimal management of MG generation units requires exact determination of constraints to describe the operation problem considering the output power generation with the least possible generation cost [14]. These are often represented as a large scale, non-convex, nonlinear, mixed-integer problems. Therefore, presenting powerful optimization algorithms to extract the best possible solution for the MGs is very important. Deterministic optimization methods are highly dependent on the system and their definition is very difficult for large complex systems. In solving optimization problems with a high-dimensional search space particularly in UC and ED problems, the deterministic and stochastic optimization algorithms do not provide a suitable solution because the search space increases exponentially with the problem size, therefore solving these problems using exact techniques (such as [15]) is not practical. On the other hand, these problems can be solved with the non-deterministic polynomial-hard (NP-hard) problem. Heuristic algorithms such as genetic algorithm [16], particle swarm optimization [17], ant colony optimization [18] and bee colony optimization [19] are some optimization methods used for unit commitment within MGs [14]. Some algorithms give a better solution for some particular problems than others. These techniques are trying to seek good (near-optimal) solutions at a reasonable computational cost without being able to guarantee either feasibility or optimality, or even in many cases to state how close to optimality a particular feasible solution is. In addition, most of these approaches have a stochastic behaviour. Therefore, it is made effort to present a deterministic heuristic search algorithm based on a swarm meta-heuristic algorithm. In [1], the design of an energy management system (EMS) is developed in order to obtain the best purchasing price in day-ahead market (DAM), as well as to maximize the utilization of existing DER and study the system stability is reported. However, no optimization approach was used in that work. Furthermore, the research work presented in this paper is a continuation of the work by the authors [15], where a framework for combining stochastic optimization, non-dispatchable resources/load demand uncertainties, and local optimization is needed.

Amongst them, special attention is paid to the optimization algorithms based on artificial bee colony (ABC) for solving optimization problems due to the population-based search capability, simplicity of implementation, adequate convergence speed and robustness [14], [20]–[23]. According to the advantages of this method, it is applied in the present paper for the optimization of MG operation in terms of performance, generation resources scheduling and economic power dispatch. For increasing effectiveness and usability in MG applications, an algorithm based on multi-period ABC (MABC) is proposed in this paper for solving energy management problems over a real MG for a day-ahead period. It is noteworthy that the proposed algorithm can also find the global optimal point in the multi-dimensional and great search space.

Another approach proposed in this paper is based on modeling the uncertainty in load demands and the generation of renewable resources. A model is presented for very short-term prediction by using artificial neural network (ANN), Markov-chain (MC) and linear regression. The proposed model utilizes ANN for primary predictions. Then, the second-order MC is applied to determine transition probability matrix (TPM) for primary prediction. Finally, a linear regression is used between the primary predictions and probability values obtained by MC for the final prediction. The MC is applied to modify the predicted values according to long-term pattern of the resource data. Applying ANN without using statistical models, increases the number of input variables for both training and utilization [24]. Further, two limitations on the use of ANN models also exist that seriously affect the prediction performance, namely, over-training and extrapolation [25]. Over-training occurs when the capacity of the ANN for training is too great, because too many training iterations is allowed. For extrapolation, the advantages of the ANNs have not been determined when they are required to perform estimation beyond available experimental data [25]. Both of these ANN imperfections are taken into account in the model proposed in this paper.

The contributions of the paper are as follows:

1) development of an intelligent algorithm based on ABC within a real MG towards supporting real time applications;

2) presentation of an algorithm based on artificial neural network (ANN) combined with Marcov chain to consider system uncertainties;
   a) prediction of wind speed in a very short-time (adequate for real-time optimization);
   b) reduction of prediction error and uncertainty of predictions;
   c) significant reduction in calculation time which is considered very critical in real-time applications.
3) experimental implementation of the proposed smart algorithm demonstrating some benefits including flexible multi-device support, fast development with a running time proper for real-time applications.

II. Algorithms implementation for EMS

The EMS proposed in this paper is depicted in Fig. 1. It comprises different units, namely ANN-MC, EMS and LEM units. As shown in Fig. 1, four different algorithms are presented for implementing EMS based on LEM by using heuristic techniques or without using any optimization method. Flexibility, good accuracy, speed in decision making and plug and play abilities of LEM unit, MCEMS, EMS-MINLP (EMS based on mixed integer non-linear programming) and EMS-PSO (EMS based on particle swarm optimization) algorithms are discussed in detail in the previous studies [1], [14], [15]. Therefore, these are not addressed in the present paper and only EMS-MABC algorithm is described.

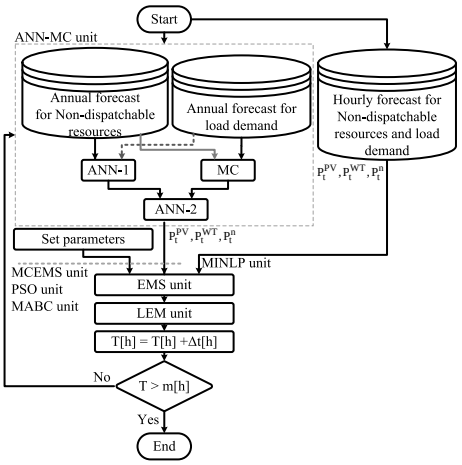

Fig. 1: Proposed algorithm for implementing EMS

A. EMS-MABC algorithm

This algorithm encompasses ANN-MC, MABC and LEM units as illustrated in Fig. 1. Since LEM unit is explained in detail in [1] and [15], only ANN-MC and MABC units are discussed bellow.

1) ANN-MC unit: In this study, MC method is applied for obtaining long-term trends in wind speed data. Thus, a simple ANN structure with the minimum number of input variables and data regulations is required for training and the over-training problem can be solved with the proposed structure. As the MC method keeps the signals long-term behavior in the memory, the error obtained from the extrapolated prediction is also reduced. As another solution for extrapolation problem, the artificial samples covering the entire range are drawn as much as possible based on the existing knowledge about the proposed problem then used for ANN initializing to ensure that most of the future prediction involves interpolation. The outline of the proposed model is shown in Fig. 2. A set of wind speed data 2.5s in a 175min period is used to improve the model accuracy for predicting wind speed up to 7.5s ahead (total of 4200 wind speed data). In Fig. 2, TPM is transition probabilities matrix for the primary prediction, forward neighborhood indices (FNI)s and Backward neighborhood indices (BNIs) are two upper/lower states and their corresponding probabilities, respectively. v_{t-k}^i is the real speed data at time t-k, and $\hat{v}_{t-k|t}$ is the predicted wind speed data for t+k and i states an index of the model i^{th} vector used in ANN-1. Also, $v_{t-1}, v_{t-2}, \cdots, v_{t-n}$ are considered as wind real speed data which are used for forming TPM by MC. In the proposed model, two ANNs are used for prediction. The first ANN (ANN-1) is applied for primary prediction and short-term obtaining of wind speed signal, where 10 real-time speed data from t to t-10 are used as input variables. Primary prediction can take place by ANN-1 for different time horizon. For training, 30 sets of data with 10 measured wind speed in each set are selected. After primary prediction, the provided TPS for the values and four other indices with primary predictions are fed as input variables to the second ANN (ANN-2). At the end, the implemented model based on two ANNs and MC method can be utilized for predicting different time horizons. Multi-layer perceptron (MLP) is used for ANN-1 which includes an input layer, a hidden layer and an output layer. In the output layer, only one neuron is used as $\hat{v}_{t-k|t}$ in which k is the time step and $\hat{v}$ is the anticipated wind speed at time t+k (calculated at time t). Because the number of neurons in each layer have an effect on the speed and network stability, sensitivity analysis shows that the structure of ANN-1 with the least mean absolute percentage error (MAPE) is equal to 5, 2 and 1 neurons for input, hidden and output layers with 30 training vectors and 0.01-0.08 learning rates. Based on the wind speed data histogram, wind speed states have become compatible with the 1m/s upper and lower limit difference of the wind speed for reaching high accuracy at an acceptable time. Based on the state matrix, it is possible to find the number of transitions from the two previous states during wind speed data sequence to the next state at time t+k. Finally, TPM is calculated. TPM is formed by using 600 wind speed data and the calculated matrix is used as primary prediction values (Fig. 2). At the beginning, Markov state is calculated for the primary prediction values by ANN-1 for one step ahead. Then, according to TPM, the probability of predicted value is calculated during the next step. This process is carried out for all of the primary predictions. It must be noted that the prediction values of the previous step are generated by ANN-1. For the final prediction, MLP has been used for ANN-2. The number of neurons in the input layer is selected by considering the calculation of time and error (maximum prediction error (MPE) and MAPE). Since ANN-2 has six input and one output

variables, the number of neurons in each layer must be located in the range of variables and the best structure for ANN-2 with the least MAPE is estimated as 3,0 and 1 neuron for the input, hidden and output layers with 10 training vector and learning rate between 0.01-0.05. In Fig. 3, the proposed model is shown for ANN-MC unit.

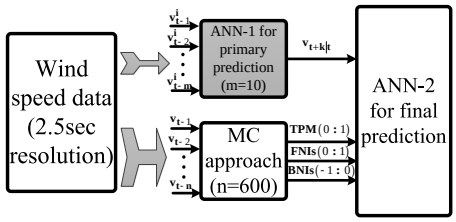

Fig. 2: General outline for the proposed model in ANN-MC unit

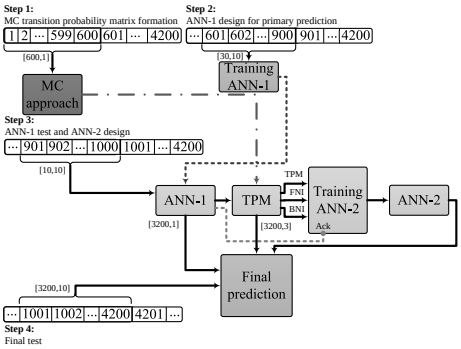

Fig. 3: Flowchart of four stages for implementation of the proposed model for ANN-MC unit

Annual pattern of non-dispatchable power generation and load demand are captured by ANN. Then, second-order MC is applied to calculate TPM. Basically in TPM formation, the non-dispatchable power generation and load demand time series are converted to power states which contain the generated and consumed powers among certain values. Based on state matrix, it is possible to find the number of transition from two preceding states in the sequence of power data to another state at time. Firstly, Markov state for primary values predicted by ANN-1 is calculated for one step ahead. Then, according to TPM, the probability of predicted value is calculated in the next step. This process is carried out for all primary predictions. It should be noted that the predicted values are produced in the previous step by ANN-1. For longer prediction horizon, transition probabilities are necessary for steps ahead. In these cases, the above TPM is multiplied in ANN-1 according to the number of time steps in the future. It is difficult to determine the relationships between the primary prediction and the coefficients obtained from MC. Since ANNs can encode complex and non-linear relations, ANN-2 is used to capture the relationships between the primary prediction and obtained probabilities. The transition probability of the predicted values state and ANN-1 output are fed to ANN-2 in order to achieve higher prediction accuracy under uncertain conditions in comparison with primary predicted values. The procedure can be summarized as follows (Fig. 3):

Step 1

TPM calculation based on 600 data points of wind speed;

Step 2

Design of ANN-1 for primary prediction by using 300 other points of wind speed data;

- Calculation of MAPE and MPE

Step 3

Implementation of MC model for testing ANN-1 and designing ANN-2 (another 100 data set);

- finding non-dispatchable and load demand data state
- evaluation of different states transition
- TPM calculation
- TPM accumulation

According to Fig. 3, ANN-1 designed in the previous step is applied for the primary prediction. Then, the TPM calculated in step 1 is used to calculate the required coefficients. ANN-2 provides six input variables of primary wind speed prediction, their transition probability values, FNI-1 and FNI-2 of the current predicted states and BNI-1 and BNI-2 of previous predicted states.

Step 4

Design of ANN-2 for secondary prediction by using ANN-1 and TPM.

Both ANNs and TPM obtained are applied steps for the final prediction.

All the above steps must be applied for different prediction time horizons.

2) MABC unit: The flowchart of MABC unit is shown in Fig. 4. The highlighted areas in this Figure are the modifications made to ABC algorithm in order to adapt it in MG application. Each response of the optimization problem has D variables. In this paper, $D = 7$ is considered including WT (P_t^{WT}), PV (P_t^{PV}), MT (P_t^{MT}), charging and discharging power ES (P_t^{ES+} and P_t^{ES-}), EWH (P_t^{EWH}) and DR (P_t^{DR}) variables. The proposed algorithm is trying to find the optimal values for the design variables that minimize the objective function. Therefore, X_t^i is defined as $X_t^i = x_t^{i,1}, x_t^{i,2}, \cdots, x_t^{i,7}$ vector. The elements are $x_t^{i,1} = P_t^{i,WT}$, $x_t^{i,2} = P_t^{i,PV}$, $x_t^{i,3} = P_t^{i,MT}$, $x_t^{i,4} = P_t^{i,ES+}$, $x_t^{i,5} = P_t^{i,ES-}$, $x_t^{i,6} = P_t^{i,EWH}$ and $x_t^{i,7} = P_t^{i,DR}$. These variables are divided into two categories of dependent ($P_t^{i,MT}$, $P_t^{i,ES+}$, $P_t^{i,ES-}$, $P_t^{i,EWH}$ and $P_t^{i,DR}$) and independent ($P_t^{i,WT}$ and $P_t^{i,PV}$) variables. Since WT and PV are non-dispatchable resources which are affected by weather conditions, MT and ES powers can be varied depending on the power generated by WT and PV and energy consumed by load. To begin, independent variables must be made considering ANN-MC unit output. It is necessary to involve target population members in program planning, implementation and evaluation of objective function. It must be checked during optimization process if the generated population members satisfy constraints or not. Then, by using valid values for these independent variables and associated constraints, dependent variables can be generated randomly. Furthermore, after selecting a food source, the onlooker bee generates a new food source. MABC unit is illustrated by a

Pseudo-code in Algorithm 1.

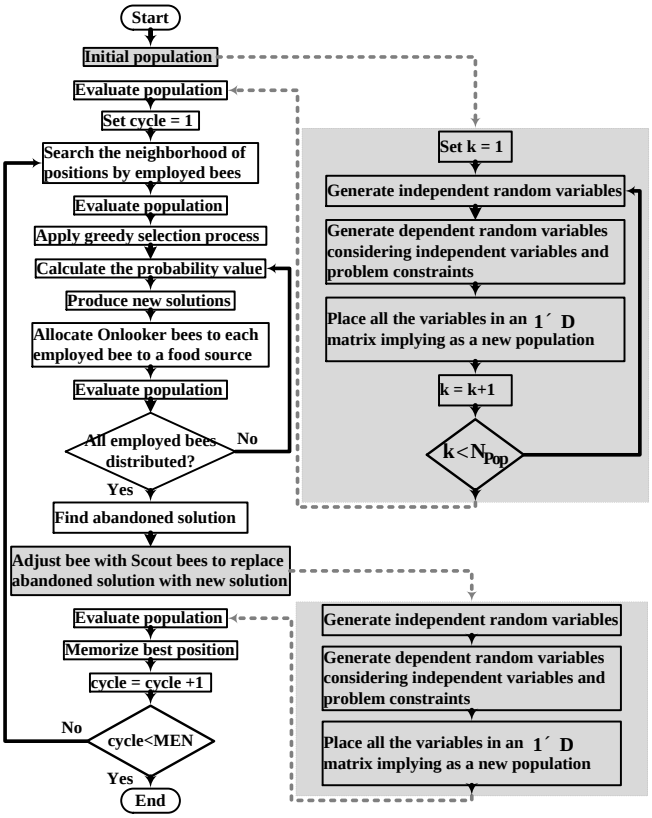

Fig. 4: The graphical representation of the process undergone in the MABC unit

III. Modified ABC algorithm

Several attempts, employing classical ABC were made in the past for solving UC. However, ABC algorithm is good at exploration but poor at exploitation. These drawbacks become more prominent in case multimodal problems having several optima. This paper presents a modified ABC algorithm for optimization problems to improve the exploitation capability of the ABC algorithm and to further improve its performance. In this paper, to improve exploitation process of classic ABC, a different probability function modifying searching mechanism has been applied to the original ABC algorithm. Probability value of selecting a food source determines the exploitation rate. In order to improve the exploitation mechanism of onlooker bees, a modified probability function has been proposed in this paper (Eq. (2)). In addition, to increase the population diversity, avoid the premature coverture as well as to improve the exploitation of classic ABC algorithm, a second modification has been proposed by using a new searching mechanism (Eq. (1)). In the first modification, the worst fitness valued solution has the best chance to local search then algorithm uses the best solution in the current population to mutate parameters in the second modification. Generally, these modifications are based on reducing the colony size; maintaining the perturbation scheme; and using a rank selection strategy for maintaining diversity. In the

Algorithm 1 MABC UNIT

Require: PV, WT and load demand profile of the MG, the initial SOC of ES and the characteristic of system.

Initialize *control parameters/ the problem specific parameters*

for $t = 0 : m$ **do** ▷ m: the number of time periods

Generate the initial population by

$$X_t^{i,j} = \underline{x}^j + \rho \times (\overline{x}^j - \underline{x}^j) \tag{1}$$

▷ $X_t^{i,j}$: j^{th} variable from the i^{th} response at time t, $i \in \{1, 2, \cdots, N_P\}$, $j \in \{1, 2, \cdots, D\}$ ▷ $\overline{x}^j$ and $\underline{x}^j$: upper and lower of component x ▷ ρ: random number in [0, 1] interval

Evaluate (Eq.(7))

cycle =1

while cycle <MCN **do** ▷ MCN: maximum cycle number

Employed bee **Generates** $x_t'^{i,j}$ by

$$x_t'^{i,j} = x_t^{i,j} + \rho' \times (x_t^{i,j} - x_t^{k,j}) \tag{2}$$

▷ $k \in \{1, 2, \cdots, N_P\}$, $k \notin i$ ▷ $x_t'^{i,j}$: new food source in the neighborhood of $x_t^{i,j}$ position

Evaluate and **apply** the greedy selection process

Onlookers **Calculate** P_t^i for $x_t^{i,j}$ by

$$P_t^i = \frac{fit_t^i}{\sum_{j=1}^{N_P} fit_t^j} \tag{3}$$

▷ fit_t^j: fitness value of i^{th} response at t

Generates $x_t'^{i,j}$ based on P_t^i

Evaluate and **apply** the greedy process

Scout **Determine** the abandoned $x_t^{i,j}$ if exist

Update it by Eq.(7)

Update the best solution acquired so far

end while

Return optimal power set-points

end for

proposed MABC, binary numbers 1 and 0 are used to indicate the status of generating units ON/OFF whereas the economic dispatch is solved using the real coded ABC. Whereas classical ABC algorithm is essentially a real-coded algorithm, thus, some modifications are needed to deal with the binary-coded optimization problem. In the proposed ABC, the relevant variables are interpreted in terms of changes of probability. The onlookers produce a modification in the position selected by it using (Eq. (1)) and evaluate the nectar amount of the new source. Improving strategy throughput by constraint based management in MABC whenever the commitment status for each time interval is generated randomly or by the modification of employed/onlooker bee′s position, dispatchable constraint must be checked as follows:

Step 1: If dispatchable resources constraints are met, then go to Step 3. Otherwise, go to next step.

Step 2: The less expensive units which are shut OFF can be identified and should be turned ON. Then go to Step 1.

Step 3: If dispatchable resources constraint is satisfied, then the maximum and minimum operating times constraints are checked for each unit. If there is any violation in the minimum up or down time constraint then a repair scheme is performed to overcome the violation.

Step 4: The modified scheme for Step 3 can effect on the dispatchable resources constraint. If the reliability level is sufficient, then return the feasible solution. Otherwise go to Step 1.

IV. Problem formulation

The problem formulation is divided into two parts which are closely connected and dependent on each other. The first part is related to the prediction error of uncertainty model and the other include MG constraints.

A. Error criteria for uncertainty consideration

The prediction error of a model is classically defined as the difference between the measured and predicted values. A horizon dependent model error $e^t_{t+\Delta t}$ is given by

$$e^t_{t+\Delta t} = P^X_{t+\Delta t} - \widehat{P}^X_{t+\Delta t} \tag{4}$$

where X denotes non-dispatchable resources and load demand entries. $P^X_{t+\Delta t}$ is the measured X power at time $t+\Delta t$, $\widehat{P}^X_{t+\Delta t}$ is the power prediction for X computed at time t. The most commonly used evaluation criterion is the MAPE defined as follows [24].

$$MAPE_k = \frac{1}{N}\sum_{t=1}^{N}(|\frac{e^t_{t+\Delta t}}{P^X_{t+\Delta t}}| \times 100) \tag{5}$$

where Δt and N describe the prediction horizon and number of prediction, respectively. It is very important to reduce MPE because a large prediction error and consequently wrong control commands may cause an unstable condition for non-dispatchable resources. MPE is calculated as [24].

$$MPE_{\Delta t} = max|\frac{e^t_{t+\Delta t}}{P^X_{t+\Delta t}}| \times 100; t = 1, \cdots, N \tag{6}$$

B. MG mathematical modeling

The system under study is considered as an islanded MG including non-dispatchable (WT and PV in this study) and dispatchable generation resources (MT in this study) and ES supplying some responsive (EWH and DR in this study)/ non-responsive loads (NRL). The optimization problem is defined as the following cost function:

$$min\sum_{t=1}^{m}(\mathbb{C}^g_t + \mathbb{C}'^g_t + \mathbb{C}^{ES-}_t - \mathbb{C}^{\ell}_t - \mathbb{C}^{ES+}_t + \Omega_t) \times \Delta t \tag{7}$$

where m is the number of the simulation periods in time interval t, $\mathbb{C}^g_t$ and $\mathbb{C}'^g_t$ are the cost of the energy generated by non-dispatchable and dispatchable resources, respectively, $\mathbb{C}^{ES+}_t$ and $\mathbb{C}^{ES-}_t$ are the energy generation cost by ES unit during charging and discharging operation modes, respectively, $\mathbb{C}^{\ell}_t$ is the cost of the energy consumed by responsive load demand (RLD) (EWH and DR are respectively termed as shiftable and controllable loads in this study) and Ω_t is the penalty cost resulting from undelivered power (UP) during the time period t. The objective of economic dispatch problem is in fact minimizing the total production cost while satisfying generation resources constraints. Ω_t is included in the objective function as a penalty cost for the MG operator to avoid undelivered power to the NRL. Each one of these costs can be calculated as follows

$$\mathbb{C}^g_t = \sum_{k=1}^{n^g} \pi^{k,g}_t \cdot P^{k,g}_t \tag{8}$$

$$\mathbb{C}'^g_t = \sum_{k=1}^{n'^g} \pi'^{k,g}_t \cdot P'^{k,g}_t \tag{9}$$

$$\mathbb{C}^{\ell}_t = \sum_{k=1}^{n^{\ell}} \pi^{k,\ell}_t \cdot P^{k,\ell}_t \tag{10}$$

$$\mathbb{C}^{ES+}_t = \sum_{k=1}^{n^{ES}} \pi^{k,ES+}_t \cdot X^{ES}_t \cdot P^{k,ES+}_t \tag{11}$$

$$\mathbb{C}^{ES-}_t = \sum_{k=1}^{n^{ES}} \pi^{k,ES-}_t \cdot (1 - X^{ES}_t) \cdot P^{k,ES-}_t \tag{12}$$

$$\Omega_t = \pi^{UP}_t \cdot P^{UP}_t \tag{13}$$

where $\pi^{k,g}_t$ and $\pi'^{k,g}_t$ are the k^{th} non-dispatchable and dispatchable resources, $P^{k,g}_t$ and $P'^{k,g}_t$ are the output power generated by the k^{th} non-dispatchable and dispatchable resources, n^g and n'^g are the number of non-dispatchable and dispatchable units installed in the MG system, Δ_t is duration of the period t, $\pi^{k,\ell}_t$ is the offer price by k^{th} RLD, $P^{k,\ell}_t$ is the output power consumed by k^{th} RLD during the time period t, π^{UP}_t is the offer price when the system is encountered UP and P^{UP}_t is the amount of power is not supplied by MG. X^{ES}_t is status of ES operation mode (i.e. X^{ES}_t=0 when ES is in the discharging mode and X^{ES}_t= 1, otherwise).

Equality and unequally constraints are formulated in the following:

- Power balance

$$\sum_{k=1}^{n^g} P^{k,g}_t + \sum_{k=1}^{n'^g} P'^{k,g}_t + \sum_{k=1}^{n^{ES}}(1 - X^{ES}_t) \cdot P^{k,ES-}_t + P^{UP}_t = P^{NRL}_t + \sum_{k=1}^{n^{\ell}} P^{k,\ell}_t + \sum_{k=1}^{n^{ES}} X^{ES}_t \cdot P^{k,ES+}_t \tag{14}$$

- non-dispatchable resources

$$0 \leq \sum_{k=1}^{n^g} P^{k,g}_t \leq \overline{P}^g \tag{15}$$

where $\overline{P}_t^g$ is the maximum power generated by non-dispatchable generation units during the time period t.

- dispatchable resources [15]
  - electricity generation unit boundaries
  - ramp-up and ramp-down limits
  - maximum and minimum operating times
- ES constraints [15], [26]–[28]
  - energy storage limits;
  - maximum charge/discharge power limit;
  - maximum charge/discharge energy stored limit;
  - energy balance in ES;
  - SOC limit;
  - ES limit.
- RLD constraints

$$P_t^{RLD} = \overline{P}_t^{RLD} \tag{16}$$

$$\sum_t P_t^{DR} = \sum_t P_t^{UP} \tag{17}$$

$$P_t^{EGP} = X_t^{ES} \cdot P_t^{ES+} + X_t^{DR} \cdot P_t^{DR} + P_t^{EWH} \tag{18}$$

$$\sum_t P_t^{EGP} = \sum_t X_t^{ES} \cdot P_t^{ES+} + \sum_t X_t^{DR} \cdot P_t^{DR} + \sum_t P_t^{EWH} \tag{19}$$

where X_t^{DR} is a binary variable indicating DR status (i.e. 1 if the request is in service and 0 otherwise). Eq. (17) guarantees that the total consumed power by DR should be equal to the total P_t^{UP} during daily operation system, whereas EGP at each interval can be supplied for charging of ES, DR and EWH as formulated in Eq. (18). In addition, the summation of consumed power by these customers should be equal to the summation of EGP during a daily operation system as shown mathematically in Eq. (19).

V. Application to Test Grid

EMS-MABC algorithm is implemented and validated experimentally over the IREC′s MG. In this MG, all the microsources with any characteristic can easily be emulated by digital signal processing. This MG is used to investigate various concepts such as control design and implementation of EMS [1], [15], [28]–[30]. A general scheme of this system including emulators is shown in Figs. 5 and 6. This MG has two non-dispatchable resources (PV and WT), a dispatchable resource (MT), and ES integrated with some responsive (EWH and DR) and NRL. Emulators specifications are presented in the previous papers [1]. Furthermore, the system has a controller that EMS-MABC algorithm should be loaded in that. To begin, the central controller receives data including generated power and load demand (P_t^{WT}, P_t^{PV} and P_t^n) provided by ANN-MC unit, SOC, and bid offers. Then, all optimal power set-point of each microsource will be dispatched to them at each time interval based on

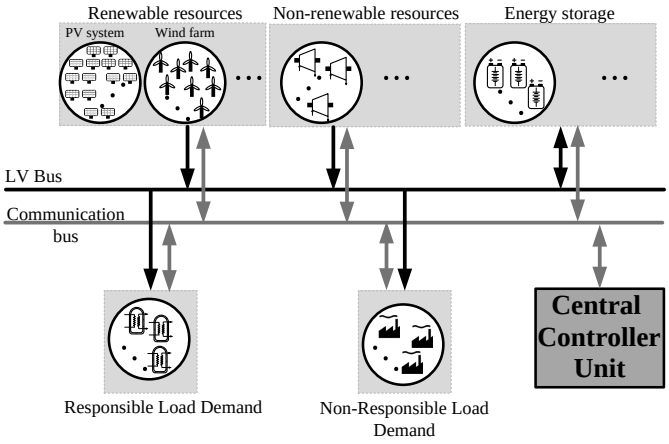

Fig. 5: Schematic of the MG system under study

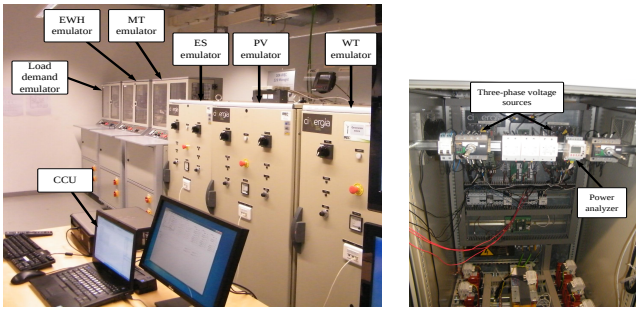

(a) IREC′s MG (b) Cabinet inside details

Fig. 6: System configuration of IREC′s MG Testbed

EMS algorithm. WT, PV and load demand profiles are shown respectively in Figs. 7(a)- 7(c) [1].

The ability of the proposed algorithm under several scenarios is considered for optimal scheduling and operation of resources, minimizing the generation cost as well as applying demand side management.

The following scenarios are studied:

- Scenario ♯1: Normal operation
- Scenario ♯2: Sudden load increase
- Scenario ♯3: Plug and play ability

VI. Results and Discussion

In this section, the results of experimental evaluation of the proposed algorithm over IREC′s MG are presented.

SOC and ES power during the 24 hour system operation are shown in Figs. 8 and 9, respectively. As it is observed in Fig. 8, during 00:00-06:00 period, SOC_t is almost always decreasing and at the end of this operation interval reached to $\underline{SOC}$. However, in EMS-MABC a part of the power needed for charging the ES is provided by MT. As a result, SOC_t' is reached about to 70% at the end of this time interval. More SOC causes the increase of the ability for supplying the loads during the rest of the system daily operation. During 06:00-12:00 period, MCEMS has already used ES for supplying a part of power shortage, while in EMS-MABC, ES is operated in the charging mode and continuing to reach $\overline{SOC}$. It is still clamped until the end of this interval. Scenarios

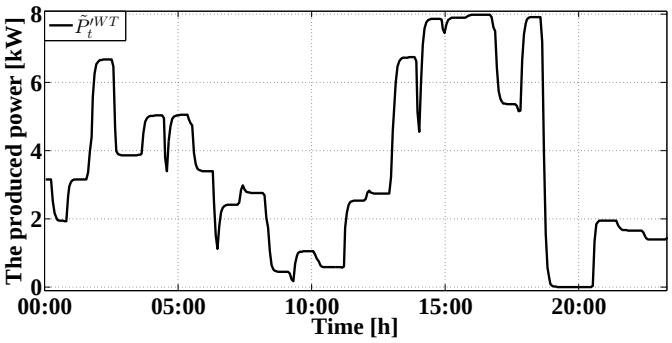

(a) WT emulator

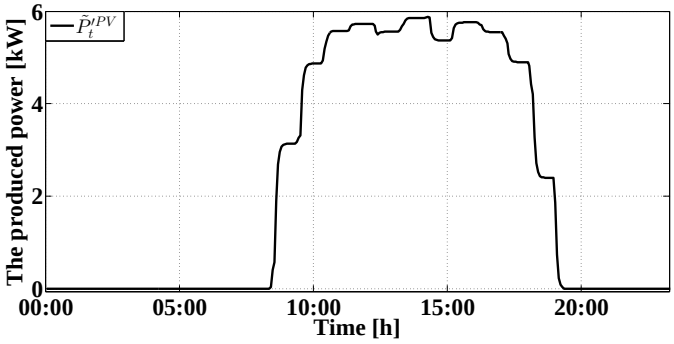

(b) PV emulator

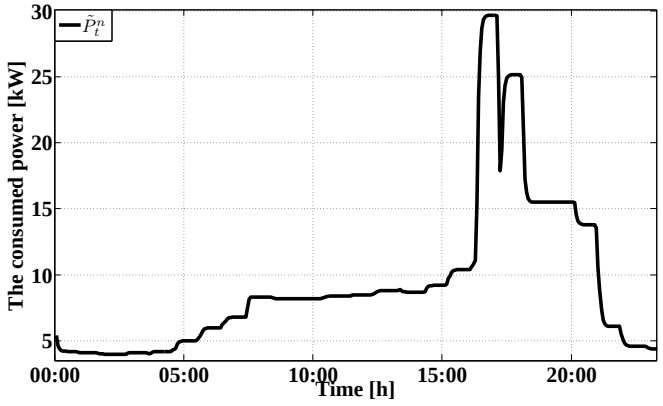

(c) Load emulator

Fig. 7: the power generated by the emulators WT, PV and load demand

♯2 and ♯3 are occurred between 12:00-18:00 period and despite in both of the algorithms MT is served and ES is fully discharged, MG is not able to completely supply the load demand. During 18:00-24:00, ES in MCEMS operates in discharging mode reaching $\underline{SOC}$. However, by proper selection of MT, ES is operated in the charging mode in EMS-MABC and at the end of this time interval, SOC is about 80%. Dispite of higher MT offer relative to ES, EMS-MABC has recognized that if it can use MT for compensating the shortage of power and meanwhile use the rest of the generated power for charging ES, the total generation cost will be minimized. In addition to cost reduction, ES stored more energy for supplying the loads in the next day.

The bar graphs of ES charging/ discharging, RLD, UP and

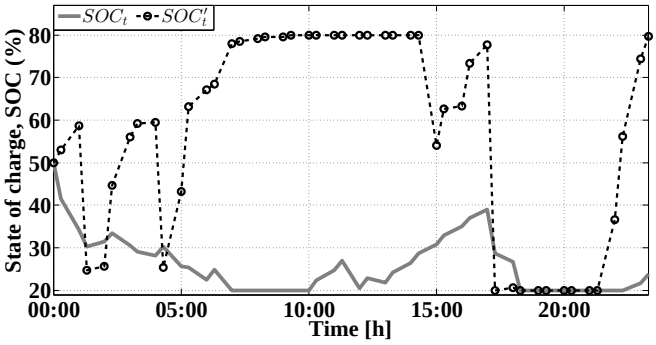

Fig. 8: SOC during system operation (Solid light-gray line indicates MCEMS algorithm. Also, dash black line with circle marker type represent output of EMS-MABC algorithm)

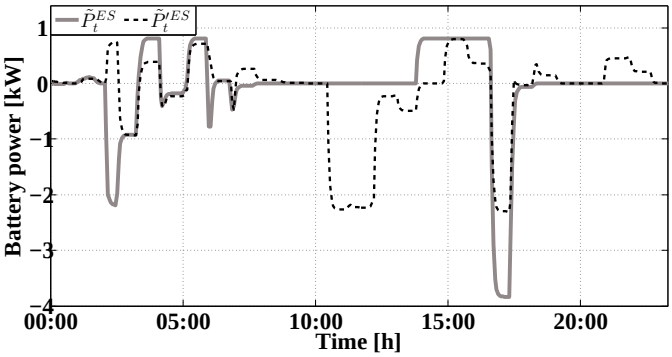

Fig. 9: Charging/discharging power of ES emulator during system operation

EGP power are shown in Fig. 10. As it is observed in both algorithms, MG is not able to supply the power required by all consumers in scenarios ♯2 and ♯3 during 12:00-18:00. UP in MCEMS is more than EMS-MABC and ES is fully discharged.

It is noticeable that in this time interval, P_t^{ES-} is about 30% more than its value in EMS-MABC. Therefore, more penalty cost due to lack of delivery of the power required by consumers should be paid. In these time intervals, λ_t^{MCP} is about 0.3 €/kWh, but when UP exists, MCP is about 0.9 €/kWh. On the other hand, EMS-MABC has significantly reduced the electricity cost by curtailing a number of consumers (when MCP is relatively high) and feeding them at other hours with cheaper MCP. EWH is mainly supplied in the afternoon for both algorithms. λ_t^{MCP} is about 37% greater than the respective value of $\lambda_t'^{MCP}$ at the same time. As it is observed in Fig. 10(a), ES in MCEMS is mainly charged with $\overline{P}^{ES+}$ power. In the time intervals in which ES operates in the charging mode, λ_t^{MCP} is about 0.49 €/kWh, while $\lambda_t'^{MCP}$ for charging ES is about 0.32 €/kWh that is approximately 34% less than the MCP in MCEMS.

For experimental evaluation, the proposed algorithms are implemented in C environment on a PC with i5-3320 M, 4 GB RAM, 2.6 GHz. Table I shows the experimental results of proposed algorithm including computation time and total generation cost which is compared with the conventional PSO method. It is clearly seen in this table that EMS-MABC

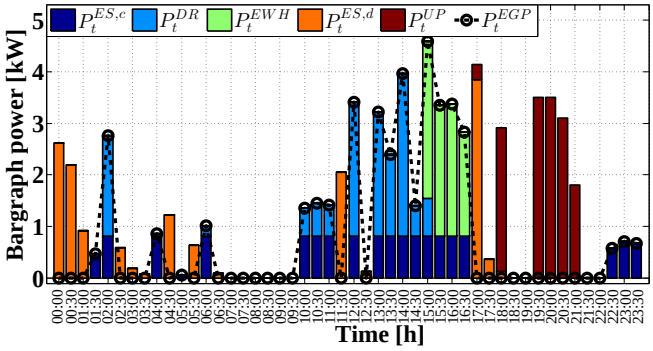

(a) MCEMS

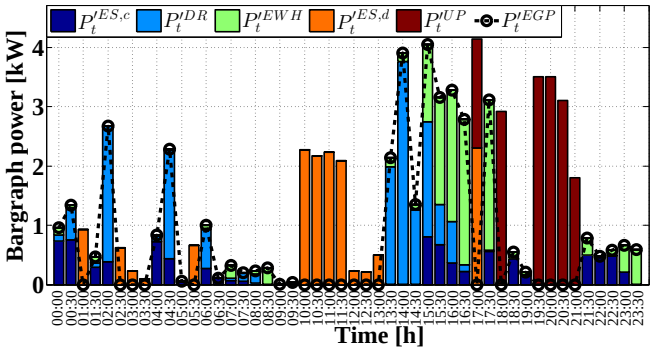

(b) EMS-MABC

Fig. 10: Bar graph related to the responsive loads power, charging/discharging ES and UP during the system 24 hours performance

TABLE I: Run time and total generation cost for case study corresponding to 100 iteration

	MABC	PSO
Execution time (S)	10.14	27.45
Total generation cost (€)	35.35	36.42
Error (%)	1.26	4.32

algorithm got the minimal total generation cost around 35.35 € and needed shorter computation time than PSO algorithm. Also, the nearest value of objective function compared to realistic method (MINLP) is achieved in MABC algorithm.

MCP during daily operation system of shown in Fig. 11. λ_t^{MCP} and $\lambda_t'^{MCP}$ during the day are respectively 0.52 €/kWh and 0.32 €/kWh that shows a 39% reduction in EMS-MABC. The maximum value of λ_t^{MCP} (1.33 €/kWh) is observed during scenario ♯2, while the maximum value of $\lambda_t'^{MCP}$ is 0.90 €/kWh and is obtained during scenarios ♯2 and ♯3. The minimum value of λ_t^{MCP} and $\lambda_t'^{MCP}$ are respectively 0.2 €/kWh and 0.13 €/kWh which are obtained for both algorithms during 00:00-06:00. MCP values during 24 hours of system operation are listed in Table II for both algorithms. As observed, MCPs in both algorithms are minimum during 00:00-06:00, so it is proper to supply more number of RLD and ES loads in this time interval. During this period, the supplied RLD and ES in EMS-MABC algorithm

TABLE II: The average value of MCP during system operation

00:00-06:00	06:00-12:00	12:00-18:00	18:00-24:00	MCP
0.62	0.49	0.56	0.57	λ_t^{MCP}
0.50	0.43	0.35	0.52	$\lambda_t'^{MCP}$

are totaly about 46% more than their values in MCEMS. As a result, these consumers are supplied with lower price. During 06:00-12:00, in both algorithms, MT is placed in service and with attention to its higher offer in comparison with other generation sources, MCP is significantly increased. Hence, RLD and ES is supplied in EMS-MABC for a proportionately less time (about 85%). During 12:00-18:00, PV is started to generate power when the sun is starting to rise and MT is gone out of service. Since PV offer is less than MT, MCP is drastically reduced. Furthermore, in this time interval, about 6% more of RLD and ES loads are supplied in MCEMS in comparison with EMS-MABC. During 18:00-24:00, MCP is maximum in both algorithms, so it is beneficial that the loads with less offers are supplied in this time interval. Only ES with highest offer is charged in MCEMS while EWH is also fed in EMS-MABC. EWH has proposed minimum offer and as a result, consumers are considerably less cost-effective for feeding their loads.

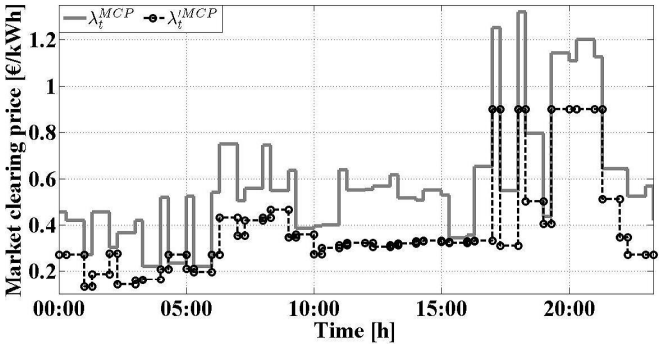

Fig. 11: MCP for each interval during the system daily performance

VII. Conclusions

In this paper, modeling of consumers′ information has been addressed by using EMS-MABC to present RLD characteristics in a DR program as well as to estimate the participation quality and commitment in a LEM structure with the aim of reducing MCP. In addition, a new concept for the virtual generation sources derived from demand resources has been introduced to estimate the optimal scheduling of generation resources and DR in an isolated MG. The DR constraints are expressed with various status flags, the information of other consumers and the excess power generated has been modeled to obtain the minimum total generation cost and less market clearing price. These points have been considered for modeling the limiting conditions for

the consumers participating in a demand response program. The optimal programing for generation scheduling combined with DR has been performed to minimize the operation cost of MG linked to customer information. This combined programming has been evaluated over a MG Testbed. Since renewable resources such as WT and PV have intermittent characteristic, approaches to analyze economic dispatch in MGs would be stochastic rather than deterministic. To take the uncertainties into account, ANN-MC method according to artificial neural network combined with Markov-chain concept is implemented.

The obtained experimental and simulation results show the reduction of the total operation cost (about 30%) also significant reduction of MCP in each time interval with adequate and real time control of DR in the proposed algorithm. The proposed approach shows more decrease in the objective function than EMS-PSO algorithm while reducing computation time.

REFERENCES

[1] M. Marzband, A. Sumper, A. Ruiz-Álvarez, J. L. Domínguez-García, and B. Tomoiagă, "Experimental evaluation of a real time energy management system for stand-alone microgrids in day-ahead markets," *Applied Energy*, vol. 106, no. 0, pp. 365–76, 2013.

[2] M. Savaghebi, A. Jalilian, J. Vasquez, and J. Guerrero, "Autonomous voltage unbalance compensation in an islanded droop-controlled microgrid," *IEEE Transactions on Industrial Electronics*, vol. 60, no. 4, pp. 1390–402, April 2013.

[3] J. Vasquez, J. Guerrero, M. Savaghebi, J. Eloy-Garcia, and R. Teodorescu, "Modeling, analysis, and design of stationary-reference-frame droop-controlled parallel three-phase voltage source inverters," *IEEE Transactions on Industrial Electronics*, vol. 60, no. 4, pp. 1271–80, April 2013.

[4] M. Savaghebi, A. Jalilian, J. Vasquez, and J. Guerrero, "Secondary control for voltage quality enhancement in microgrids," *IEEE Transactions on Smart Grid*, vol. 3, no. 4, pp. 1893–902, Dec 2012.

[5] M. Savaghebi, A. Jalilian, J. C. Vasquez, and J. M. Guerrero, "Secondary control scheme for voltage unbalance compensation in an islanded droop-controlled microgrid," *IEEE Transactions on Smart Grid*, vol. 3, no. 2, pp. 797–807, June 2012.

[6] Y. Zhang, N. Gatsis, and G. Giannakis, "Robust energy management for microgrids with high-penetration renewables," *IEEE Trans. Sustain. Energy*, vol. 4, no. 99, pp. 1–10, 2013.

[7] Y. Levron, J. Guerrero, and Y. Beck, "Optimal power flow in microgrids with energy storage," *IEEE Trans. Power Syst.*, vol. 28, no. 3, pp. 3226–34, 2013.

[8] T. Wu, Q. Yang, Z. Bao, and W. Yan, "Coordinated energy dispatching in microgrid with wind power generation and plug-in electric vehicles," *IEEE Trans. Smart Grid*, vol. 4, no. 99, pp. 1–11, 2013.

[9] F. Farzan, S. Lahiri, M. Kleinberg, K. Gharieh, F. Farzan, and M. Jafari, "Microgrids for fun and profit: The economics of installation investments and operations," *IEEE Power Energy Mag.*, vol. 11, no. 4, pp. 52–58, 2013.

[10] M. Tasdighi, H. Ghasemi, and A. Rahimi-Kian, "Residential microgrid scheduling based on smart meters data and temperature dependent thermal load modeling," *IEEE Trans. Smart Grid*, vol. PP, no. 99, pp. 1–9, 2013.

[11] N. Bottrell, M. Prodanovic, and T. Green, "Dynamic stability of a microgrid with an active load," *IEEE Trans. Power Electron.*, vol. 28, no. 11, pp. 5107–19, 2013.

[12] Y. Simmhan, V. Prasanna, S. Aman, A. Kumbhare, R. Liu, S. Stevens, and Q. Zhao, "Cloud-based software platform for big data analytics in smart grids," *IEEE Comput. Sci. Eng.*, vol. 38-47, no. 99, pp. 1–10, 2013.

[13] C. M. Colson, M. H. Nehrir, R. Sharma, and B. Asghari, "Improving sustainability of hybrid energy systems part II: Managing multiple objectives with a multiagent system," pp. 46–54, 2013.

[14] M. Marzband, "Experimental validation of optimal real-time energy management system for microgrids," PhD Thesis, Departament d'Enginyeria Elèctrica, EU d'Enginyeria Tcnica Industrial de Barcelona, Universitat Politècnica de Catalunya, 2013.

[15] M. Marzband, A. Sumper, J. L. Domínguez-García, and R. Gumara-Ferret, "Experimental validation of a real time energy management system for microgrids in islanded mode using a local day-ahead electricity market and MINLP," *Energy Conversion and Management*, vol. 76, no. 0, pp. 314–22, 2013.

[16] B. Zhao, X. Zhang, J. Chen, C. Wang, and L. Guo, "Operation optimization of standalone microgrids considering lifetime characteristics of battery energy storage system," in *IEEE Transactions on Sustainable Energy*, 2013, pp. 1–10.

[17] Y. Y. Hong, M. C. Hsiao, Y. R. Chang, Y. D. Lee, and H. C. Huang, "Multiscenario underfrequency load shedding in a microgrid consisting of intermittent renewables," *IEEE Transactions on Power Delivery*, vol. 28, no. 3, pp. 1610–17, 2013.

[18] W. Najy, H. Zeineldin, and W. Woon, "Optimal protection coordination for microgrids with grid-connected and islanded capability," *IEEE Transactions on Industrial Electronics*, vol. 60, no. 4, pp. 1668–77, 2013.

[19] M. V. Kirthiga, S. A. Daniel, and S.Gurunathan, "A methodology for transforming an existing distribution network into a sustainable autonomous micro-grid," *IEEE Transactions on Sustainable Energy*, vol. 4, no. 1, pp. 31–41, 2013.

[20] A. K. Basu, "Microgrids: Planning of fuel energy management by strategic deployment of CHP-based DERs- an evolutionary algorithm approach," *International Journal of Electrical Power & Energy Systems*, vol. 44, no. 1, pp. 326–36, 2013.

[21] S. A. Taher and R. Bagherpour, "A new approach for optimal capacitor placement and sizing in unbalanced distorted distribution systems using hybrid honey bee colony algorithm," *Electrical Power and Energy Systems*, vol. 49, no. 1, pp. 430–48, 2013.

[22] K. Chandrasekaran and S. Simon, "Multi-objective unit commitment problem with reliability function using fuzzified binary real coded artificial bee colony algorithm," *IET Generation, Transmission Distribution*, vol. 6, no. 10, pp. 1060–73, 2012.

[23] A. El-Zonkoly, "Multistage expansion planning for distribution networks including unit commitment," *IET Generation, Transmission Distribution*, vol. 7, no. 7, pp. 766–78, 2013.

[24] S. A. Pourmousavi and M. M. Ardehali, "Very short-term wind speed prediction: A new artificial neural network-markov chain model," *Energy Conversion and Management*, vol. 52, no. 1, pp. 738–45, 2011.

[25] C. Yin, L. Rosendahl, and Z. Luo, "Methods to improve prediction performance of {ANN} models," *Simulation Modelling Practice and Theory*, vol. 11, no. 3-4, pp. 211–22, 2003.

[26] M. Marzband, A. Sumper, M. Chindriş, and B. Tomoiagă, "Energy management system of hybrid microgrid with energy storage." Suceava, Romania: *The International Word Energy System Conference (WESC)*, June 2012.

[27] M. Marzband and A. Sumper, "Implementation of an optimal energy management within islanded microgrid." Cordoba, Spain: International Conference on Renewable Energies and Power Quality (ICREPQ), April 2014.

[28] M. Marzband, M. Ghadimi, A. Sumper, and J. L. Domínguez-García, "Experimental validation of a real-time energy management system using multi-period gravitational search algorithm for microgrids in islanded mode," *Applied Energy*, vol. 128, no. 0, pp. 164–74, 2014.

[29] A. Ruiz-Álvarez, A. Colet-Subirachs, F. Álvarez-Cuevas Figuerola, O. Gomis-Bellmunt, and A. Sudriá-Andreu, "Operation of a utility connected microgrid using an IEC 61850-based multi-level management system," *IEEE Transactions on Smart Grid*, vol. 3, no. 2, pp. 858–65, june 2012.

[30] A. Colet-Subirachs, A. Ruiz-Alvarez, O. Gomis-Bellmunt, F. F. Alvarez-Cuevas, and A. Sudria-Andreu, "Centralized and distributed active and reactive power control of a utility connected microgrid using IEC 61850," *IEEE Transactions on system journal*, vol. 6, no. 1, pp. 58–67, 2012.